Theoretical Indications of Singular Structural and Electronic Features of Laves-Phase $CaLi_2$ Under Pressure

Ji Feng,[1] N. W. Ashcroft,[2,*] and Roald Hoffmann[1,†]

[1]*Department of Chemistry and Chemical Biology, Cornell University, Ithaca, 14853-1301 New York, USA*
[2]*Laboratory of Atomic and Solid State Physics, Cornell University, Ithaca, 14853-2501 New York, USA*

(Received 14 January 2007; published 11 June 2007)

In spite of the presence of ostensibly simple constituents, $CaLi_2$ should be a very peculiar material under pressure. Its two 1-atmosphere polymorphs each undergo a structural bifurcation on densification to structures compressed or elongated in one lattice direction. A Hume-Rothery–type mechanism is proposed to account for the indicated lattice distortion. The narrowing of valence bands under pressure in this material, a large density of states at the Fermi level, and the expected high dynamical scales also hint at superconductivity.

DOI: 10.1103/PhysRevLett.98.247002 PACS numbers: 74.70.Ad, 62.50.+p, 71.20.Dg, 74.62.Fj

The bandwidths of the occupied valence states of both calcium ($r_s = 3.26$ at 1 atm [1]) and lithium ($r_s = 3.25$) have been found to notably decrease upon sufficient increase in density [2,3]. Might stoichiometric compounds of Li and Ca also exhibit such peculiarities? The Hume-Rothery rules governing alloying and structural changes in relatively simple metals provide a guidepost. The stability, or nesting, condition on electron concentration (reflected in a concentration dependent Fermi wave vector k_F) is $k_F/(K/2) \sim 1$ (where K is the magnitude of the shortest lattice vector of the appropriate Brillouin zone). This yields an effective valence very close to 1.5 and, accordingly, we are led to consider $CaLi_2$.

The only intermetallic compound between Ca and Li at atmospheric pressure, $CaLi_2$ is a Laves phase with two polymorphs, the cubic $MgCu_2$ type [4] and the hexagonal $MgZn_2$ type [5] (Fig. 1). The cubic phase has four interpenetrating sets of layers of lithium kagomé nets, while the hexagonal phase features a unique set of kagomé layers. The Ca atoms form a diamond network in the cubic phase and a hexagonal diamond network in the hexagonal phase.

Several highly unusual features emerge from our work. (1) A predicted sequence of unusual structural lattice bifurcations in both the hexagonal and cubic phases, the consequence of latent zone planes that become activated under pressure. Some of these involve local elongation in one direction while the overall density increases, and it has some generality. (2) A quite radical departure at high density of the electronic structure of $CaLi_2$ from free-electron behavior. The elevated density of states (DOS) at the Fermi level, coupled with the expected high dynamical scale of Li as well as the possibility of favorable interlayer phonons, points to potential superconductivity of $CaLi_2$ under pressure.

We apply density functional theory with a plane-wave basis set, as implemented in VASP for static lattices. All electrons in Li and the $3p$ and $4s$ electrons of Ca are treated self-consistently, and the other core states of Ca are described by pseudopotentials. Perdew-Berke-Ernzerhof functionals [6] are used in conjunction with projector-augmented wave pseudopotentials [7,8].

A sequence of fascinating structural deformations is calculated for $CaLi_2$. The hexagonal symmetry of the $MgZn_2$-type polymorph is maintained up to over 200 GPa. However, this phase undergoes a significant *lattice bifurcation* at pressures >47 GPa, showing at each volume two energy minima corresponding, respectively, to $c/a >$ and $< \sqrt{8}/3$ (the value adopted in $CaLi_2$ at atmospheric pressure) [9]. These two distorted structures are referred to as hexagonal elongated (HE) and hexagonal compressed (HC) phases and for $r_s = 2.42$ are shown in Figs. 2(a) and 2(b), respectively. In the HC phase ($c/a = 1.58$, $p = 53$ GPa) three of the Li-Li separations around a hexagonal hole of the kagomé net are longer than the other three. As a result, if only the closest Li atoms are connected by lines, we see chains of trigonal bipyramids of Li atoms. At $r_s = 1.91$ ($p = 212$ GPa), the c/a ratio of the HC phase is as low as 1.29. The HE phase ($c/a = 1.86$, $p = 52$ GPa) shows a layered character due to the (relative) lattice elongation, as illustrated in Fig. 2(b). The unexpected elongation increases with pressure until $r_s = 2.00$ (176 GPa), where $c/a = 2.24$.

The computed double-well potential energy surface [10] along the c/a coordinate at fixed density ($r_s = 2.42$) is shown in Fig. 2(c). At this density, the energy difference between the HC and HE phases is of the same order of magnitude as the uncertainty in the calculated energy ($\sim$1 meV/$CaLi_2$). The energy barrier between the two minima, 4–6 meV, is well below the dynamical scale of Li, whose Debye energy is $\sim$36 meV/atom [11]. This suggests (a) the interesting possibility of lattice fluctuation, through *cooperative tunneling*, and (b) that restoration of finite masses to both Ca and Li may well result in some exceedingly interesting thermally driven phase transitions, and ensuing transport properties. At higher pressures, the energy well on the *elongated* side deepens compared to the compressed one, though the shallow well on the com-

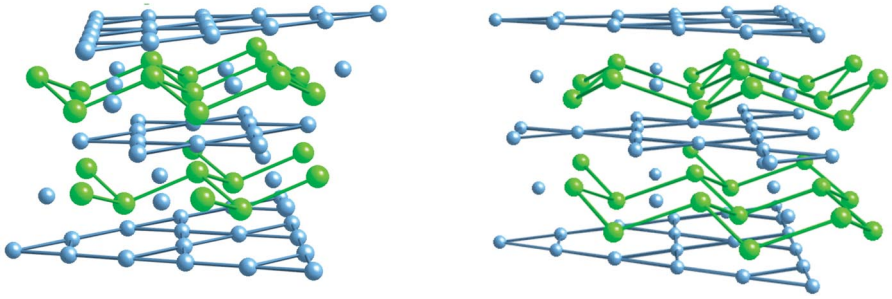

FIG. 1 (color). Left: structure of cubic $MgCu_2$-type $CaLi_2$; right: $CaLi_2$ in hexagonal $MgZn_2$-type structure. Blue: Li; green: Ca. These views emphasize the layered arrangement of kagomé nets of Li atoms and puckered sheets of Ca.

pressed side persists to the highest pressures we have studied.

Cubic $CaLi_2$ goes through successive symmetry-lowering Martensitic distortions as the pressure increases. The underlying lattice changes from fcc, to body-centered tetragonal (bct), and then to body-centered orthorhombic (bco) with compression ($Fd\bar{3}m \Rightarrow I4_1/amd \Rightarrow I\bar{4}2d \Rightarrow I2_12_12_1$). At 15 GPa, two energy minima emerge, with c/a ratios greater and smaller than $\sqrt{2}$ (the value corresponding to a cubic cell). An orthorhombic, albeit small, distortion begins at the same point [12]. We will call these two distorted phases cubic elongated (CE) and cubic compressed (CC), including the orthorhombic modifications. In the CC phase at $r_s = 2.42$ [46 GPa, $c/\sqrt{ab} = 0.96$; Fig. 2(d)] the diamond network of Ca is compressed along the fourfold helical axis, becoming a β-tin-like network. We also note a local rotation of the Li_4 tetrahedral clusters, in addition to the compression along c direction. The Li_4 clusters in the CE phase at the same density (50 GPa, $c/\sqrt{ab} = 1.59$) are also rotated, but this time stretched along the c direction as shown in Fig. 2(e). The calculated enthalpies of the most important structures are shown in Fig. 3.

What causes the deformations? Mott and Jones attributed the stability of cubic diamond, having the same symmetry and electron count as cubic $CaLi_2$, to the large zone bounded by (220) zone planes [13,14]. Here, the (311) Fourier component of the self-consistently screened one-electron pseudopotential (V_{311}) is of similar magnitude as the strongest (220) component (V_{220}), but the former zone planes do not yet touch the Fermi sphere. Upon compressive tetragonal distortion, 16 of these (311) planes will move closer to the free-electron Fermi surface, while 8 will move farther away. Since the free-electron energy corresponding to $(\frac{3}{2}\,\frac{1}{2}\,\frac{1}{2})$ is well within $|V_{311}|$ of the free-electron E_F [15], it is expected that such a distortion will be stabilizing, and, as a consequence, there is an inherent lattice instability to tetragonal distortion.

By examining a model local pseudopotential we find that $|V_{311}|$ rises rapidly with increasing density [15,16]. In addition, the occupied valence band width of $CaLi_2$ grows very slowly with density and at high pressure actually *drops*. Therefore, the lattice instability, as measured by the increasing $V_{\mathbf{K}}/E_F$, is expected to increase with density. At a critical point, as the energy penalty is overcome, the distortion is realized [16].

In the CC phase at $r_s = 1.92$, chains of Li and Ca atoms can be identified, as depicted in Fig. 4(a). At this pressure the lattice vectors a and b are significantly different and the lattice is decidedly orthorhombic ($I2_12_12_1$). The Ca atoms form zigzag chains, while the Li atoms form helices with 4 atoms per full turn [17]. The low-symmetry $CaLi_2$ phase

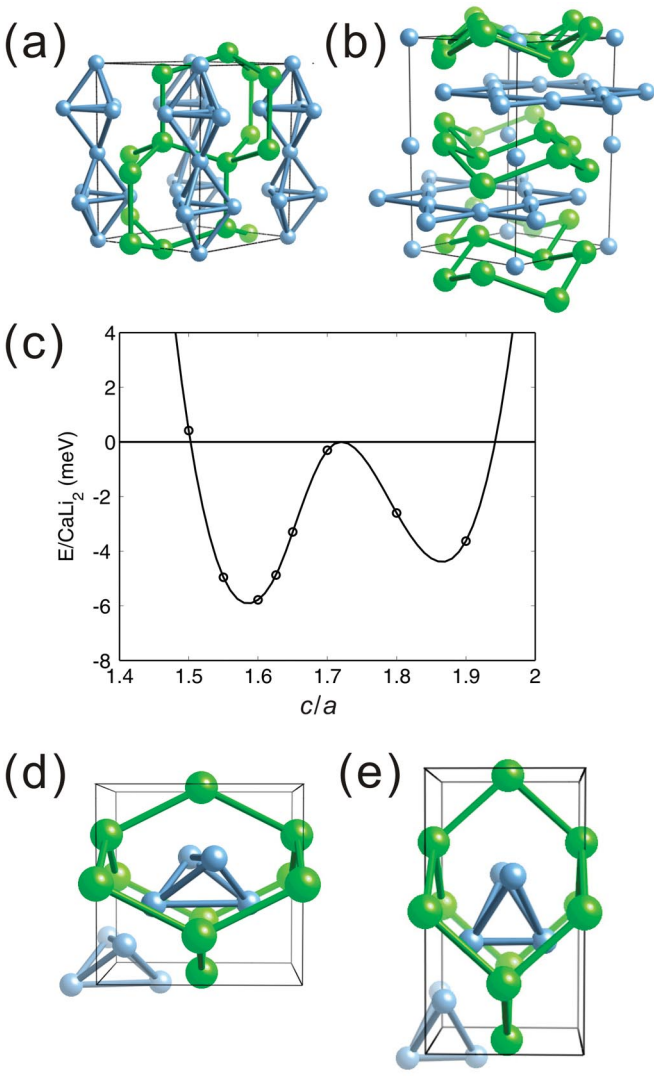

FIG. 2 (color). (a),(b) The structures of HC and HE at $r_s = 2.42$, respectively. (c) The constant-volume potential energy surface of the hexagonal phase at this volume. CC (d) and CE (e) structures at $r_s = 2.42$.

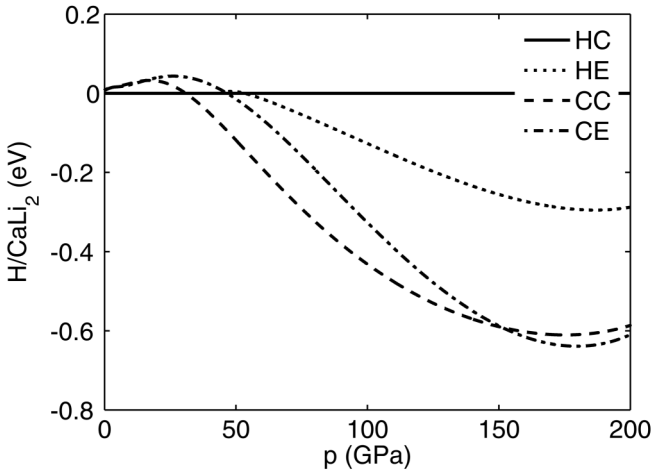

FIG. 3. Enthalpies of the competitive structures of $CaLi_2$ under pressure.

has two regions of high density of valence electrons [Fig. 4(b)]. The first is near the Ca ions, possibly because of the higher effective nuclear attraction acting on valence electrons and the nodal structure of the core wave functions. The second high valence density region is *between* Li helices. This interstitial electron pocket itself forms a helix, propagating perpendicularly to the front face of the unit cell shown. Regions near the Li ions and between the nearest Li-Li neighbors show low valence density. The origin of the peculiar distribution of valence density under high pressure is the exclusionary effect of core states, as discussed by Neaton and Ashcroft [2,18].

Structural complexities in hand [19], we can look at the surprising electronic structure of these phases [20]. Bandwidth should normally increase with overlap of atomic orbitals from neighboring atoms, and that overlap, in general, increases with reduced internuclear separations [21]. In $CaLi_2$ the band width actually drops with increasing density, after a sluggish initial rise (Fig. 5 inset). At $r_s = 2.08$ ($p = 139$ GPa), the bandwidth attains its minimum value, at 3.44 eV, only a third of the free-electron expectation. A similar astounding narrowing of valence bands has recently been observed in Li, Ca, and Na [2,3,22]. Thus the electronic peculiarities of the elements persist in their intermetallic compounds. And we also find that they are independent of the specific structure or distortion $CaLi_2$ adopts.

The DOS of CC with l projections at this density ($r_s = 2.08$) is shown in Fig. 5 [8]; this DOS is most un-free-electron-like, with massive peaks at the bottom of the occupied valence manifolds. The s, p, and d orbtials contribute over the entire energy range of the occupied valence bands. The occupied valence levels on Ca are overwhelmingly d in character, with some s character and rather small p contributions [8].

To the best of our knowledge, $CaLi_2$ has not been scrutinized for possible superconductivity. This, we believe, is a likely property of $CaLi_2$, under high pressure if not at 1 atm. Two aspects are of obvious importance in this context—the attractive electron-phonon-electron coupling and the electron-electron repulsion. For the former, it would appear the situation should be no less favorable overall than it is for the constituent elements themselves, except that additional pairing strength may be derived from a multiplicity of intergrouping modes (the equivalent of interplanar modes in MgB_2 [23]). The far more important issue concerns the electron-electron terms, which are critically dependent on the details of electronic structure in a multiband situation as here [24].

The density of states clearly plays an important role for these terms; we find that at the Fermi level, N_F in $CaLi_2$ rises until $p = 8.8$ GPa ($r_s = 2.89$), when the hexagonal structure is more stable. Then N_F begins to drop, and at 26 GPa the Fermi level sits in a narrow but rather deep pseudogap. $CaLi_2$ is, however, unlikely to become semimetallic at this pressure, as the gap is so narrow that it can be washed out by dynamical effects. After transformation to the CC phase above 31 GPa, the Fermi level continues to

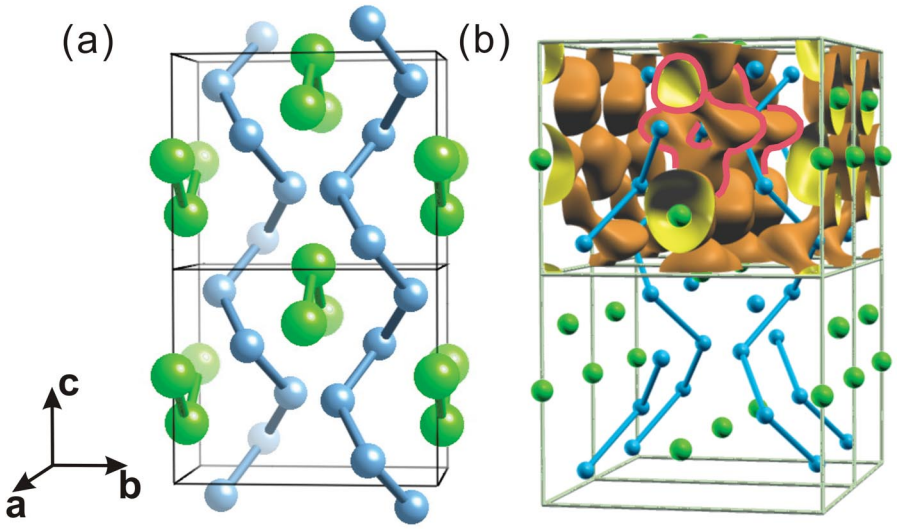

FIG. 4 (color). (a) Perspective view of the CC phase at $r_s = 1.92$ and (b) electron density distribution. In (b) the electron density isosurface is shown only for upper two cells. The yellow side of the surfaces faces the higher density region, while the orange faces the lower. The boundaries of one of the pockets of electrons in the interstitial region between Li helices are highlighted by red lines. The isosurface cutoff value is 0.28 $e/Å^3$.

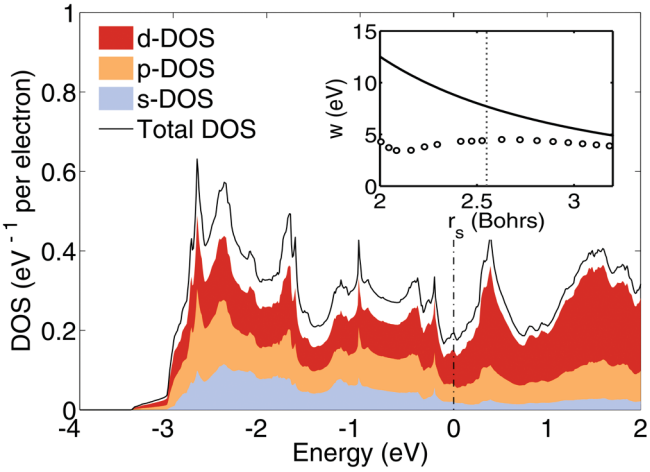

FIG. 5 (color). The DOS with l projections of the CC phase at $r_s = 2.08$. Inset: The variation of the computed width (w) of occupied valence band (open circles) as a function of r_s. The solid line is the free-electron expectation of the valence bandwidth. The vertical dotted line marks the density of phase transition from HC to CC.

fall in a pseudogap, but at higher pressures, the N_F value increases again due to the band narrowing. At 202 GPa the CE phase is most stable and attains an N_F value of 0.22 per electron volt per electron, 1.8 times the free-electron expectation at this density. These high DOS values, in addition to the lightness of Li, may potentially lead to significant superconductivity, though it is clear that the phonon structure, and the possibility of propitious interlayer phonons (as occur in MgB_2), has yet to be established.

We see in $CaLi_2$ that the presence of constituents otherwise regarded as "simple" can nevertheless lead in certain combinations to behavior of quite striking complexity, and perhaps even favorable to ordered electronic states. This suggests more generally that a broader investigation of the wide class of intermetallics, especially those incorporating the lighter elements (and under low temperature and high pressure conditions) may be of considerable interest.

We are grateful to the National Science Foundation for the support of the work through Research Grants No. CHE-0613306 and DMR-0601461 and The Petroleum Research Fund of the American Chemical Society for Grant No. ACS-PRF-44853. We also thank the Ohio Supercomputer Center for computer time, and Dr. Richard Hennig for valuable help.

*Electronic address: nwa@ccmr.cornell.edu
†Corresponding author.
Electronic address: rh34@cornell.edu

[1] The free-electron sphere radius is defined as $r_s \equiv (3/4\pi n)^{1/3}$, n being the valence electron concentration.
[2] J. B. Neaton and N. W. Ashcroft, Nature (London) **400**, 141 (1999).
[3] S. Lei, D. A. Papaconstantopoulos, and M. J. Mehl, Phys. Rev. B **75**, 024512 (2007).
[4] D. Fischer and M. Jansen, Z. Anorg. Allg. Chem. **629**, 1934 (2003).
[5] E. Hellner and F. Laves, Z. Kristallogr. **105**, 134 (1943).
[6] J. P. Perdew, K. Burke, and M. Ernzerhof, Phys. Rev. Lett. **77**, 3865 (1996).
[7] G. Kresse and J. Joubert, Phys. Rev. B **59**, 1758 (1999).
[8] See EPAPS Document No. E-PRLTAO-98-025723 for auxiliary material to this Letter. For more information on EPAPS, see http://www.aip.org/pubservs/epaps.html.
[9] Lattice bifurcations have been computed for some materials. For example, indium is predicted to have similar two minima on the potential energy surface at ambient pressure, which converge under high pressure. See A. S. Mikhaylushkin *et al.*, Phys. Rev. Lett. **92**, 195501 (2004); see also some discussions in V. F. Degtyavera, Phys. Usp. **49**, 369 (2006).
[10] Because of the hexagonal symmetry, the c/a ratio and unit cell volume are enough to determine the cell shape. Hence, we first optimize the atom positions at fixed c/a at fixed volume. Then a single point calculation is performed to obtain the total energy.
[11] A. C. Evans, J. Mayers, and D. N. Timms, J. Phys. Condens. Matter **6**, 4197 (1994).
[12] Because of the additional orthorhombic distortion, the values of $c/\sqrt{ab}$ are used as indicators of lattice elongation or compression along the c direction.
[13] N. F. Mott and H. Jones, *The Theory of the Properties of Metals and Alloys* (Dover, New York, 1958).
[14] The indexing of reciprocal lattice points and planes here is based on the conventional cubic supercell of the fcc lattice. For a Fourier component to be nonzero, the following must be satisfied because of the space group symmetry: h, k, and l must be all even or all odd; if h and/or $k = 0$, $h + k + l$ must be an integral multiple of 4.
[15] N. W. Ashcroft, J. Phys. C **1**, 232 (1968). For the core radius of the pseudopotential R_C we use 1.74 and 1.06 bohr for Ca and Li, respectively.
[16] J. Feng, N. W. Ashcroft, and R. Hoffmann (to be published).
[17] For calibration, the Ca-Ca and Li-Li separations in their elemental structures are 3.94 and 3.10 Å, respectively, and in 1 atm cubic $CaLi_2$, 3.84 and 3.13 Å, respectively.
[18] In essence, at high enough density neighboring ionic cores begin to overlap. In this regime, the valence electrons are squeezed out of the internuclear region between nearest neighbors, into interstitial regions.
[19] Though we feel we have explored carefully the possible distortions from 1 atm structures of $CaLi_2$, it is of course possible that there are as yet some undiscovered and quite different structures.
[20] For electronic structure of $CaLi_2$ at ambient pressure, see M. J. Zhu, D. M. Bylander, and L. Kleinman, Phys. Rev. B **54**, 14 865 (1996), and references therein.
[21] Departures from this, for example in p-p σ overlap and s-p σ overlap, exist.
[22] J. Neaton and N. W. Ashcroft, Phys. Rev. Lett. **86**, 2830 (2001).
[23] J. M. An and W. E. Pickett, Phys. Rev. Lett. **86**, 4366 (2001).
[24] C. F. Richardson and N. W. Ashcroft, Phys. Rev. B **55**, 15130 (1997).